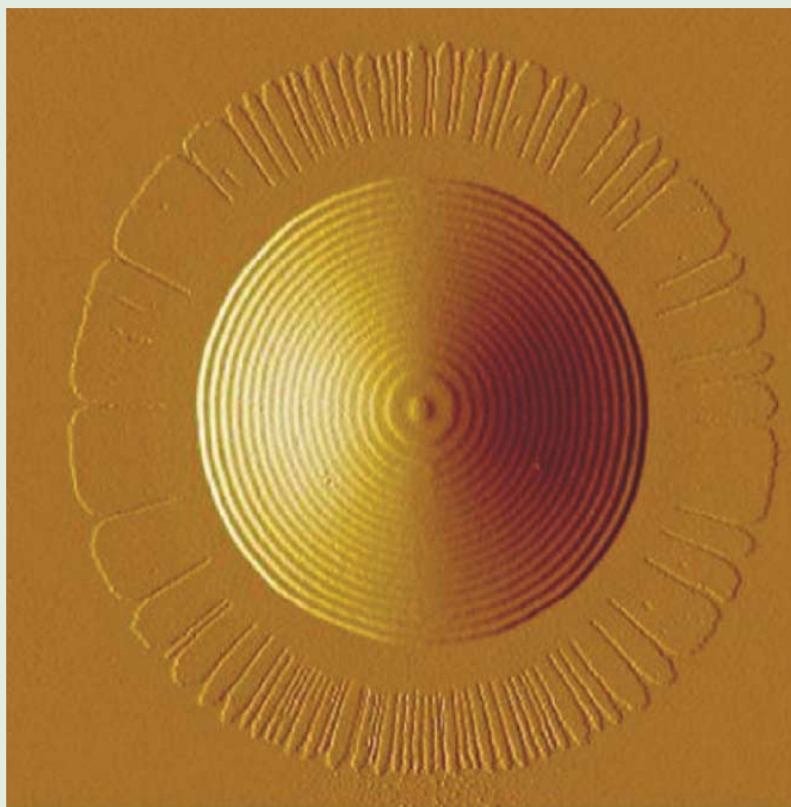


# PHYSICAL REVIEW LETTERS

Articles published week ending  
17 NOVEMBER 2006

Volume 97, Number 20



Member Subscription Copy  
Library or Other Institutional Use Prohibited Until 2011



Published by The American Physical Society

## Droplet Shape of an Anisotropic Liquid

Andrew B. Croll,<sup>1</sup> Michael V. Massa,<sup>1</sup> Mark W. Matsen,<sup>2</sup> and Kari Dalnoki-Veress<sup>1,\*</sup>

<sup>1</sup>*Department of Physics & Astronomy and the Brockhouse Institute for Materials Research, McMaster University, Hamilton, ON, Canada*

<sup>2</sup>*Department of Mathematics, University of Reading, Whiteknights, Reading, United Kingdom*

(Received 2 June 2006; published 17 November 2006)

We investigate how a droplet of a complex liquid is modified by its internal nanoscale structure. As the liquid passes from an isotropic disordered state to an anisotropic layered morphology, the droplet shape switches from a smooth spherical cap to a terraced hyperbolic profile, which can be modeled as a stack of thin concentric circular disks with a repulsion between adjacent disk edges. Our ability to resolve the detailed shape of these defect-free droplets offers a unique opportunity to explore the underlying physics.

DOI: [10.1103/PhysRevLett.97.204502](https://doi.org/10.1103/PhysRevLett.97.204502)

PACS numbers: 47.20.Hw, 61.25.Hq, 68.03.Cd, 68.08.Bc

Consider a simple fluid droplet on a solid substrate. In the absence of gravity or for small droplets, the shape is governed by the surface tension requirement of a minimal area and results in a spherical cap. The *contact angle* (the angle between the liquid-air and liquid-substrate interface at the three-phase contact line) depends on the three interfacial tensions in the system according to Young's equation [1]. Droplets of rain on a leaf are a familiar example and can be particularly striking in the case of *superhydrophobic* surfaces (with very high contact angles) like a lotus leaf [2,3]. The simple picture of a spherical droplet becomes more complex in the case of an anisotropic liquid [4], where there is some underlying order or on substrates with some lateral order [5]. Here we show that, when diblock copolymers form an ordered liquid with a lamellar structure, droplets are found to exhibit a *hyperbolic* shape. This unusual droplet shape, which can be understood from a simple model, switches to a spherical cap once the ordered structure is lost (i.e., upon passing through the order-disorder transition). While deviations from a spherical droplet are of general fundamental interest, there is also great technological potential given that the hyperbolic shape is highly regular, controllable, and switchable. Furthermore, the wide variety of existing block-copolymer nanostructures [6] implies a rich assortment of possible droplet shapes, all of which could be utilized as building blocks for nanotechnology.

Diblock copolymers are long chain molecules comprised of two chemically distinct parts (i.e., blocks) covalently bonded together. The general chemical incompatibility of the two components imparts the molecules with amphiphilic behavior that drives them to self-assemble into ordered nanostructures, where the unlike blocks reside in separate domains. The connectivity of the blocks limits the length scale of the domains to that of the molecules ( $\sim 10$  nm), and a complex interplay between the internal interfacial tension and chain stretching causes the domains to adopt morphologies with long-range periodic order. The geometry of the morphology transforms from lamellar to gyroid to cylindrical to spheri-

cal as the ratio of the block lengths deviates from one [6–8]. Although the unlike blocks are confined to separate domains, they still maintain liquidlike mobility and thus can be classified as a structured fluid. However, the melt transforms to an amorphous liquid when the temperature is increased above the order-disorder transition (ODT), where entropy dominates the energetic benefits of nanophase separation. Alternatively, the disordered state can be brought about by reducing the molecular weight ( $M_w$ ) of the molecules, because the energy cost of removing a block from its preferred domain is proportional to its size.

During the last few decades there has been significant effort to study diblocks at surfaces and interfaces [8–20]. This focus is in large part due to fundamental interest in the interdependence of surfaces or interfaces and nanostructure but it is also motivated by the technological importance of self-assembling nanostructures. Potential applications can be found in enhancing material properties, patterning, photonics, lab-on-a-chip devices, information storage, and many others, provided one can control morphology and also the orientation of morphologies (see, for example, ordering by solvent evaporation [21], ordering by substrate topography [22], and ordering by electric fields [23,24]). Understanding wetting/dewetting of diblock copolymers on a substrate is paramount to the coupling of pattern formation on two different length scales: those of dewetting ( $\sim 10$   $\mu$ m) and nanophase separation ( $\sim 10$  nm) [14–20]. It was first suggested by Fredrickson that due to the preferential interaction of an interface with one of the blocks there could be induced ordering at the substrate interface even above ODT [9]. Recent experimental work on ordering in thin films above ODT have been carried out by Green and co-workers [20]. In the cases where there is a stronger affinity for one of the blocks and the substrate, a symmetric diblock will form lamellae which order parallel to the substrate, thereby minimizing the interfacial energy.

Typically fluids that do not wet a substrate form spherical cap droplets. However, the shape of nonequilibrium droplets as they are spreading on the substrate can deviate

from the simple spherical cap. In experiments on simple fluids [25] and liquid crystals [26], as well as molecular dynamics on short chain molecules [27] it was found that the spreading droplet can be terraced. Equilibrium droplets which exhibit no flow can also show terracing, but as a result of an underlying anisotropy in a complex fluid like liquid crystals and block copolymers [10,14,28–30]. We find that droplets of symmetric diblock copolymer self-assemble into stacks of concentric circular disks with decreasing radii, again forming terraced profiles. However, we focus on the overall profile of the droplets, similar to previous work on smectic liquid crystal droplets [4]. The relative ease of imaging the terraces of diblock droplets contrasts with liquid crystal droplets where uncertainty about the actual nanostructure and nonequilibrium effects provide further challenges [30]. The droplet profiles we observe are *not* spherical, but a nearly conical shape, which can be understood from a simple model and is described by a hyperbola. Interestingly, the profiles revert to a spherical shape, when the diblock melt loses its internal lamellar structure as  $M_w$  is reduced or temperature is increased beyond the ODT.

The polymer used in this work is symmetric monodisperse poly(styrene-methyl methacrylate) (PS-PMMA) obtained from Polymer Source (Dorval, Quebec). The range of total (sum of both blocks) number-averaged molecular weights extends from  $M_n = 21$  to 104 kg/mol (see Table I), and spans both sides of the bulk ODT [31]. The substrates were electronic grade Si wafers with the native oxide layer present, which were cleaned by supercritical  $\text{CO}_2$  (Applied Surface Technologies) and UV-Ozone in order to remove surface contaminants. The polymer was “dusted” onto the clean Si and then annealed at 180 °C under vacuum ( $\sim 10^{-6}$  Torr) for long times ( $\sim 100$  h). Annealing well above the glass transition temperature ( $\approx 100$  °C) of both polymer blocks ensures that the polymer can nanophase separate and reach an equilibrium droplet shape. Droplet morphologies were obtained with atomic force microscopy (AFM) in tapping mode. Both topographic and error signal images were collected. The error signal, roughly the derivative of the topography, was used to highlight the edges of lamella. Each step of the terrace is a diblock bilayer arranged *A-B/B-A* in order to minimize the interfacial tension of the system. For the PS-PMMA system the PMMA block has a greater affinity for the

substrate and wets the substrate, while the PS block has a lower surface tension (a condition termed asymmetric wetting [8,20]). The minimum in the free energy of the system is obtained with a half lamella (diblock monolayer) at the substrate followed by full lamellae (diblock bilayers) forming the sequence: Si/PMMA-PS/PS-PMMA PMMA-PS/etc. Lamellar heights,  $L$ , of the diblock bilayer were measured with AFM and found to be in good agreement with expected values (see Table I) [7,31].

Figure 1 shows an AFM image of the error signal of a PS-PMMA(29.4 k) diblock droplet (the *total*  $M_n$  of the diblock is indicated in brackets). The image reveals several important features. (1) The terracing is very clear, and each step corresponds to a diblock bilayer. (2) The rings are almost equally spaced, indicating that the droplet has a nearly conical shape, in contrast with the usual spherical cap. (3) The first layer of the droplet is a monolayer and spreads beyond the base of the bulk of the droplet. The monolayer exhibits a clear fingering pattern. (4) The near perfect circularity of the disks strongly implies that the disks are in equilibrium.

The monolayer can be treated separately. It exhibits slow continuous growth driven by the strong tendency for

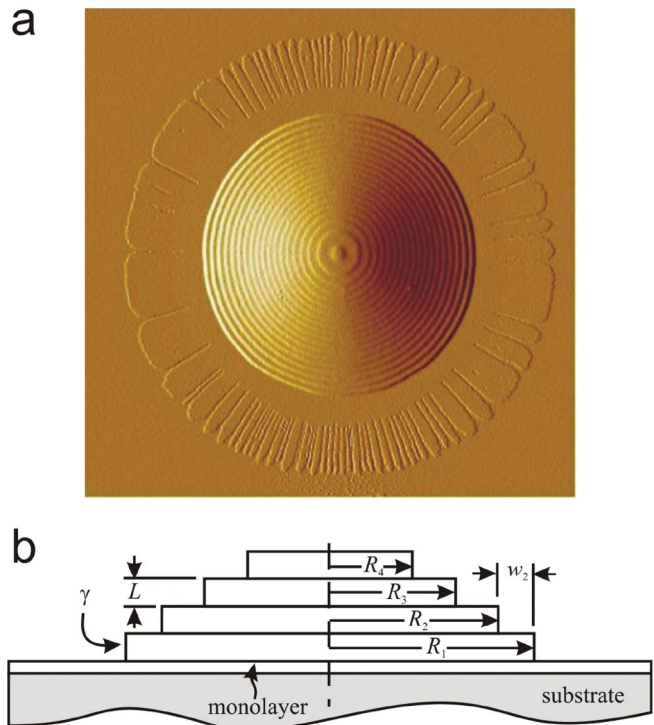


TABLE I. Molecular weights  $M_n$ , polydispersity index PI, and lamellar thickness  $L$  of the diblocks used.

$M_n(\text{PS})$ (kg/mol)	$M_n(\text{PMMA})$ (kg/mol)	PI	$L$ (nm)
10.5	10.5	1.05	$14.6 \pm 0.8$
13.4	13.6	1.05	$18.0 \pm 0.4$
15.6	13.8	1.05	$19.0 \pm 2.0$
19.3	19.3	1.07	$21.6 \pm 1.4$
27.3	28.3	1.09	$27.0 \pm 1.2$
52.0	52.0	1.09	$62.0 \pm 3.0$

FIG. 1 (color). (a) Atomic force microscopy error signal. In this  $32 \times 32 \mu\text{m}$  scan of a diblock droplet PS-PMMA(29.4 k), each ring corresponds to one lamella (diblock bilayer). The droplet has the morphology of a stack of concentric disks with increasing diameter towards the substrate. We note that the error signal tracks vertical features faithfully. The lack of detail in the horizontal fingers is due to the horizontal scan direction, and the sensitivity of the signal to *changes* in height. (b) Schematic of an ordered droplet denoting the relevant parameters: bilayer thickness  $L$ , disk radii  $R_i$ , edge tension  $\gamma$ , and terrace widths  $w_i$ .

PMMA to wet the substrate, with the bulk of the droplet acting as the reservoir from which it acquires new material. The fingering pattern is complex and dependent on both the temperature at which the sample is annealed as well as the  $M_w$  and will be the subject of a further publication. Because the monolayer spreads very slowly in comparison with the time scale on which the droplet shape is established (the time scales differ by more than 2 orders of magnitude), we can consider the bulk of the droplet to be in equilibrium on a static monolayer brush. Ultimately, if one waits a sufficient number of days, the monolayer will spread to such an extent so as to consume the entire droplet, since the minimum energy state is to cover the entire substrate with a layer of PMMA.

The behavior of the bilayers can be understood in terms of the simple model depicted in Fig. 1. This model assumes that the monolayer forms a relatively static PS surface, upon which  $n$  bilayers adjust their respective radii,  $R_i$ , so as to minimize their total free energy,

$$\frac{F}{2\pi} = \gamma \sum_{i=1}^n R_i + \sum_{i=2}^n R_i U(w_i).$$

The PS-air tension of the horizontal surfaces (including that of the monolayer carpet) is omitted because their combined area remains fixed. The only variation in area occurs due to the vertical steps; this part of the PS-air surface energy is combined in  $\gamma$  along with all the other energy costs of forming an edge to the bilayer. The last term of the free energy represents a repulsion between adjacent edges and depends on the terrace width  $w_i = R_{i-1} - R_i$ . The source of the repulsion is conceptually simple. Of course, the terraces will not exhibit the sharp idealized steps depicted in Fig. 1(b). Their equilibrium shape will be dictated by a competition between the air-PS tension, which tends to smooth out sharp corners, and the effective elasticity of the bilayers, which favors a uniform thickness [7]. For large isolated terraces, this competition will select a preferred profile with some characteristic length scale over which the bilayer disk acquires its preferred uniform thickness,  $L$ . When the separation between terraces,  $w_i$ , becomes less than this length scale, their shapes will be forced to deviate from the preferred profile causing a rise in the free energy. This excess energy represents the effective interaction,  $U(w_i)$ , responsible for the edge-edge repulsion. We find that the droplet shape is not particularly sensitive to the details of this repulsion, and choose the simple form  $U(w_i) = U_0 \exp(-w_i/w_0)$ , where  $U_0$  and  $w_0$  are fitting parameters. Naturally, the free energy must be minimized with respect to  $n$  and the  $R_i$  under the constraint that the total volume,  $V = \pi L \sum_{i=1}^n R_i^2$ , of the droplet remains fixed. We search for the equilibrium droplet shape by stepping through each value of  $n$  and introducing a Lagrange multiplier (i.e., pressure),  $P$ , which allows us to minimize  $\Omega = F - PV$  with respect to  $R_i$  as if there is no constraint.

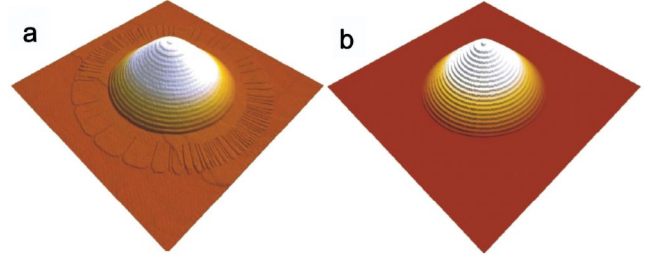


FIG. 2 (color). (a) Three-dimensional rendering of the diblock droplet shown in Fig. 1. The droplet has a diameter of  $17.6 \mu\text{m}$ . (b) The output of a best fit of the model to the data. To facilitate comparison, the same surface rendering is used.

In Fig. 2 we show AFM topography data as well as a best fit of the model to the data (the parameters  $L = 19.0 \text{ nm}$ ,  $V = L1.68 \times 10^4 \mu\text{m}^2$ , and  $R_1 = 8.78 \mu\text{m}$ , are fixed to their experimentally determined values. The fitting parameters are  $w_0/L = 1$  and  $U_0/\gamma = 1.1 \times 10^6$ ). The model is in very good agreement with the data and seems to capture all the essential physics. Numerically the location of the edges predicted by the model fall *exactly* on a hyperbola. Hence, droplets of an anisotropic fluid of this type form a hyperbolic cap, rather than the spherical cap for an isotropic fluid. This is very clear in Fig. 3 where a circle and hyperbola are fit to a droplet in the disordered and ordered state. As first predicted by Fredrickson [9], we also observe some ordering induced by the substrate for temperatures above ODT as can be seen as a small step at the droplet base in Fig. 3(a). To differentiate between the ordered and disordered droplet in a quantitative manner, the profile can be fit to the generic equation  $0 = Ax^2 + Bxy + Cy^2 + Dx + Ey + F$ . If the droplet is a spherical cap, the discriminant,  $\Delta = B^2 - 4AC < 0$ , while for a hyperbolic  $\Delta > 0$ . Measurements at  $180^\circ\text{C}$  were carried

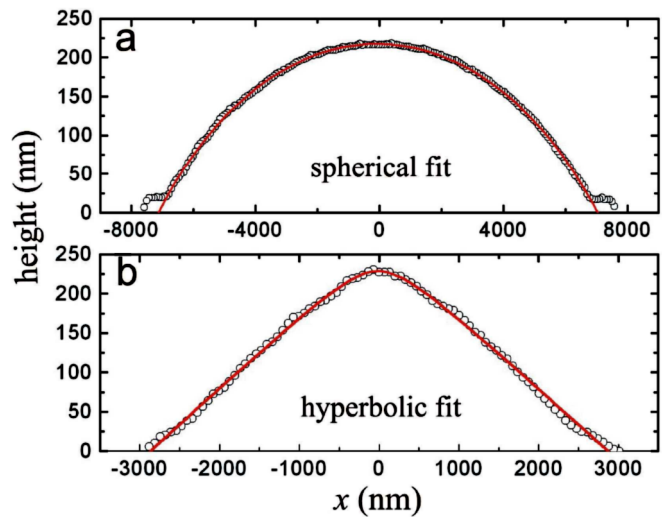


FIG. 3 (color online). Droplet profiles in the amorphous and ordered state. (a) AFM profile and fit to an amorphous spherical cap droplet PS-PMMA(27.0 k), and (b) an ordered hyperbolic droplet PS-PMMA(55.6 k).

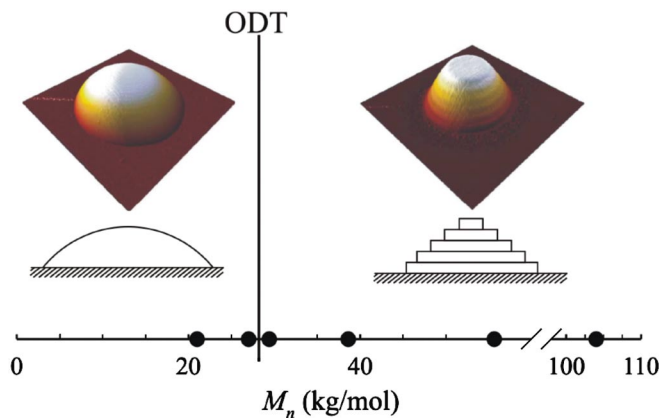


FIG. 4 (color). Phase diagram of the droplet order as a function of the total molecular weight at a temperature of 180 °C.

out for droplets with  $M_n$  ranging from 21 kg/mol to 104 kg/mol (see Table I). Using the discriminant to distinguish between the ordered and disordered droplets we obtain the results shown in Fig. 4. In changing the total  $M_n$  of the symmetric diblock from 27.0 kg/mol to 29.4 kg/mol, the system passes from being disordered to being ordered, which is consistent with the bulk ODT observed at  $M_n \approx 28$  kg/mol [31].

Here we have shown that an anisotropic liquidlike a diblock copolymer can form droplets which deviate from the classical spherical cap. An ordered droplet will orient its lamellae along the substrate because of a preferential interaction between the substrate and one of the blocks. There are two competing interactions which lead to the hyperbolic profile: (1) the edge tension which drives material from a higher (smaller) disk into a lower (larger) disk—analogueous to a small soap bubble in contact with a

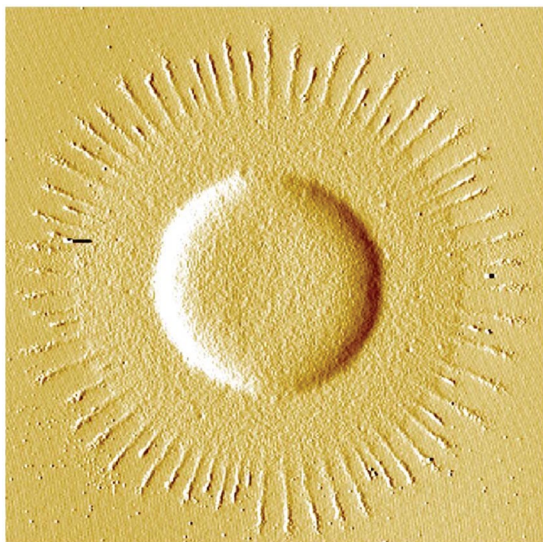


FIG. 5 (color). Error signal of a “droplet” consisting of a single bilayer disk. The  $20 \times 20 \mu\text{m}$  AFM scan of a diblock droplet PS-PMMA(29.4 k) shows a single bilayer disk on a monolayer carpet. There is a well-defined periodic fingering instability associated with the spreading monolayer.

large bubble and (2) the edge repulsion which prevents two adjacent edges from coming too close to each other. The process of smaller disks emptying into larger disks continues, with very slow kinetics compared to defining the hyperbolic shape, making an equilibrium treatment reasonable. An extreme example of this is shown in Fig. 5. In this final stage of the morphology only one bilayer disk remains on a monolayer surface which undergoes a fingering instability as it spreads onto the substrate.

The authors thank Günter Reiter and An-Chang Shi for valuable discussions. Financial support from NSERC, PREA, CFI, and OIT of Canada are gratefully acknowledged.

\*Electronic address: dalnoki@mcmaster.ca

- [1] P.G. de Gennes, F. Brochard-Wyart, and D. Quéré, *Capillarity and Wetting Phenomena* (Springer-Verlag, Berlin, 2004).
- [2] R. Blossey, *Nat. Mater.* **2**, 301 (2003).
- [3] A. Otten and S. Herminghaus, *Langmuir* **20**, 2405 (2004).
- [4] J. Bechhoefer and P. Oswald, *Europhys. Lett.* **15**, 521 (1991).
- [5] H. Gau *et al.*, *Science* **283**, 46 (1999).
- [6] F.S. Bates and G.H. Fredrickson, *Phys. Today* **52**, No. 2, 32 (1999).
- [7] M.W. Matsen, *J. Phys. Condens. Matter* **14**, R21 (2002).
- [8] M.J. Fasolka and A.M. Mayes, *Annu. Rev. Mater. Res.* **31**, 323 (2001).
- [9] G.H. Fredrickson, *Macromolecules* **20**, 2535 (1987).
- [10] B.L. Carvalho and E.L. Thomas, *Phys. Rev. Lett.* **73**, 3321 (1994).
- [11] K. Binder *et al.*, *J. Phys. II* **7**, 1353 (1997).
- [12] R. Limary and P.F. Green, *Langmuir* **15**, 5617 (1999).
- [13] P. Busch *et al.*, *Macromolecules* **36**, 8717 (2003).
- [14] D. Ausserre *et al.*, *J. Phys. II* **3**, 1485 (1993).
- [15] M.S. Turner *et al.*, *J. Phys. I* **5**, 917 (1995).
- [16] P.F. Green and R. Limary, *Adv. Colloid Interface Sci.* **94**, 53 (2001).
- [17] R. Limary *et al.*, *Eur. Phys. J. E* **8**, 103 (2002).
- [18] P. Müller-Buschbaum *et al.*, *Macromolecules* **35**, 2017 (2002).
- [19] I. Podariu and A. Chakrabarti, *J. Chem. Phys.* **118**, 11 249 (2003).
- [20] P.F. Green, *J. Polym. Sci., Part B: Polym. Phys.* **41**, 2219 (2003).
- [21] S.H. Kim *et al.*, *Adv. Mater.* **16**, 2119 (2004).
- [22] R.A. Segalman *et al.*, *Phys. Rev. Lett.* **91**, 196101 (2003).
- [23] E. Huang *et al.*, *Nature (London)* **395**, 757 (1998).
- [24] T. Thurn-Albrecht *et al.*, *Adv. Mater.* **12**, 787 (2000).
- [25] F. Heslot *et al.*, *Nature (London)* **338**, 640 (1989).
- [26] S. Betelú *et al.*, *Phys. Rev. E* **59**, 6699 (1999).
- [27] J. de Coninck *et al.*, *Phys. Rev. Lett.* **74**, 928 (1995).
- [28] M.P. Valignat *et al.*, *Phys. Rev. Lett.* **77**, 1994 (1996).
- [29] R. Lucht and Ch. Bahr, *Phys. Rev. Lett.* **85**, 4080 (2000).
- [30] P. Oswald and L. Lejček, *Eur. Phys. J. E* **19**, 441 (2006).
- [31] T.P. Russell, R.P. Hjelm, and P.A. Seeger, *Macromolecules* **23**, 890 (1990).